DEGENERATIVE CHANGES IN THE STRUCTURE OF NEUROMUSCULAR JUNCTIONS OF *MANDUCA SEXTA* DURING METAMORPHOSIS

By MARY B. RHEUBEN

Department of Anatomy, College of Veterinary Medicine, Michigan State University, East Lansing, MI 48824-1316, USA

Summary

During the degenerative processes that precede and accompany metamorphosis of the larval mesothoracic dorsal longitudinal muscles of *Manduca sexta*, the motor nerves and neuromuscular junctions undergo a variety of structural changes that are largely secondary to the changing morphologies of their respective glia. In the central region of the main motor nerve, the multiple layers of glial processes surrounding each of the large axons withdraw, leaving them apposed. In the peripheral region of the main motor nerve and in the secondary and tertiary nerve branches supplying the muscle, the outer glial processes of the nerve sheath and those that loosely wrap accompanying small neurosecretory axons all swell. Phagocytic cells and cells of unknown function invade the outer region of the nerve. In the neuromuscular junctions, the glial cells withdraw their processes from a complicated interdigitation with processes from the muscle fiber and from their relationship with the nerve terminal. As degeneration proceeds, this allows a greater area of contact between each nerve terminal and the muscle fiber. Within each junction there is a mixture of both functional and non-functional regions and active zones, as determined by both thin-section and freeze-fracture observations. No correlation was found between the degree of degeneration of a neuromuscular junction and its association with a particular muscle fiber or its position on the fiber relative to the origin or insertion.

Introduction

During metamorphosis, the slow muscles of the lepidopteran larval dorsal mesothorax degenerate and are replaced by fast muscles appropriate to power the wing strokes of the adult. The nervous system undergoes considerable rearrangement, but many of the motor neurons innervating the larval dorsal longitudinal muscles are retained and go on to innervate the adult muscles (Casaday and Camhi, 1976; Rheuben and Kammer, 1980). Up until about 12 h after the pupal ecdysis, the larval nerves, neuromuscular junctions and muscle fibers of this

particular set of muscles continue to function; stimulation of the nerve generally evokes an excitatory junction potential (EJP) and some degree of muscle contraction (Sonea and Rheuben, 1992). As the pupal period continues, the distal branches of the larval nerves to the mesothoracic dorsal longitudinal muscles appear to die back to a central region where the anlagen for the future adult muscle is forming, and new nerve branches grow out to form new neuromuscular junctions (Heinertz, 1976; Stocker and Nüesch, 1975, for the moth *Antheraea polyphemus*; M. B. Rheuben, unpublished observations).

In the other papers of this series (Sonea and Rheuben, 1992; I. M. Sonea, M. B. Rheuben and C. Young, in preparation; Rheuben, 1992) we have described the physiological changes and the changes in muscle fiber structure associated with degeneration of the larval mesothoracic dorsal longitudinal muscles of *Manduca sexta* during the late larval and early prepupal periods. When muscles of these stages were compared physiologically, the most notable changes associated with degeneration were an unexpected *increase* in amplitude of a single EJP during the early stages followed by a decline in amplitude towards the end of observable neurotransmission, a dramatic lengthening in the time course of some EJPs, a decline in resting potentials of the muscle fibers, and an increased likelihood that the nerve or its secondary branches would fail to conduct an action potential to the terminal, particularly at high stimulus frequencies. Long-term potentiation was absent or severely decreased in degenerating neuromuscular junctions.

Structurally, the first-day pupal muscle fibers showed diminished cross-sectional areas and increased perimeters compared with day 2 fifth-instar larval fibers. Over the prepupal period and the first day of the pupal period, large numbers of granules or droplets were formed within the muscle sarcoplasm and apparently exocytosed. It appeared as though the basal lamina around the muscle fiber was being removed by phagocytic hemocytes. Mitochondria degenerated and oxygen-carrying tracheoles withdrew from the muscle. In combination, the above ultrastructural changes suggested an explanation for the observed decline in resting potential and suggested that an effect on the cable properties of the muscle fiber, and subsequently on the amplitude and time course of the excitatory junction potential, might be expected (Rheuben, 1992).

The degeneration of neuromuscular junctions has been examined ultrastructurally after nerve transection in a variety of species (for example, Birks *et al.* 1960, frog; Miledi and Slater, 1970, rat; Ko, 1981, frog; Rees and Usherwood, 1972, locust; Wood and Usherwood, 1979, cockroach). In all of these species, degeneration of the nerve terminal was accompanied by changes in structure of the glial cells which normally invest it and form an integral part of the neuromuscular junction.

In this paper, we have compared the ultrastructure of the motor nerve and the neuromuscular junctions of the AB and C muscles in normal fifth-instar larvae with those from degenerating prepupal and pupal muscles by examining features which might relate to the physiological findings and which would compare to

previous results. Using transmission electron microscope (TEM) and freeze-fracture techniques, we examined the nerve terminal itself for changes in the structures related directly to transmitter release, and we paid special attention to the supporting glial structures when looking for changes comparable to those reported in denervated muscles.

Materials and methods

Tobacco hornworms [*Manduca sexta* Linnaeus)] were raised from eggs kindly provided by the Insect Hormone Laboratory, Department of Agriculture, Beltsville, MD. Larvae were fed an artificial diet (Yamamoto, 1969) and kept at 26°C on a 16 h:8 h L:D cycle.

The anesthesia, dissection and mounting of animals studied electrophysiologically prior to fixation have been described by Sonea and Rheuben (1992). For routine fixations, the larvae were anesthetized by chilling, cut parasagitally, pinned out flat with the gut ligated, and submerged in fixative at room temperature for 30 min. Intact pupae were injected with 5–10 ml of fixative for 30 min. After this initial period of fixation, individual muscle bundles were dissected free, preferably including the cuticular attachments at both ends, and submerged in vials of fresh fixative for an additional 1.5 h, followed by osmication, dehydration and embedding. Thin sections were stained for 2 h with 10 % uranyl acetate in 50 % methanol, followed by 5 min in Reynold's lead citrate.

Two different primary aldehyde fixation protocols were used. The first, with $0.2 \, \mathrm{mmol \, l^{-1}}$ calcium at all steps, contained 4 % paraformaldehyde and 1 % glutaraldehyde in Millonig's phosphate buffer. The second was formulated to be Ca^{2+}-free, with a Ca^{2+}-free presoak, until after the first 10 min of fixation, when $0.1 \, \mathrm{mmol \, l^{-1}} \, Ca^{2+}$ was included. The constituents are listed in Rheuben (1992). This second protocol gave better definition of the electron-lucent glial processes in transmission electron microscopy.

The muscles to be fixed and adjacent identifying landmarks such as tracheoles were drawn *in situ* and electrophysiological recording sites were noted when applicable. After embedding, the muscle piece was re-drawn and fibers were identified and numbered within the block face from thick sections. This was feasible because each of these larval muscles has only 9–15 very large muscle fibers. These drawings were used to identify specific muscle fibers and neuromuscular junctions in TEM sections.

Specimens prepared for freeze-fracture were fixed using the first protocol for 2 h, rinsed in phosphate buffer, and slowly transferred to 23 % glycerol, where they remained for approximately 45 min. Small groups of fibers were cut and mounted on gold stubs before being frozen in Freon slush and stored in liquid nitrogen. Complementary replicas were obtained in a Balzers 360M, adherent tissue was digested away in warm Purex bleach, and the tissue was rinsed in distilled water and photographed at 60 kV in a JEOL 100 CX transmission electron microscope (TEM).

In this part of our investigations of the development of the dorsal longitudinal muscles, seven fifth-instar larvae, eight prepupae and 28 pupae were examined ultrastructurally.

The images from the degenerating junctions were categorized into five stages (see Results), being scored blindly (without knowledge of age or experiment number) by two independent observers. Each junctional profile was examined at 14 500× and 65 750×. Some were scored twice, but none differed by more than one stage, and there was reasonable consistency between the observers. The junctions were then identified and the results tabulated to look for trends either within different parts of the same junction or between junctions in different regions of the muscle.

Results

Degeneration of the main motor nerve supplying the dorsal mesothoracic muscles

Nerve IIN1, after giving off a major sensory branch to the tubercles of the skin and to thoracic proprioceptors, contains 11–13 large axons in the region adjacent to muscles AB and C. The nerve trunk, viewed in cross section, can be divided into two regions: a cohesive core containing the axons ensheathed tightly by glial and perineurial cells and a loose collar region consisting of several thick layers of basal lamina, tracheoles and tracheoblasts, glial and 'other' cell processes and small neurosecretory axons (Fig. 1).

The core region undergoes quite striking changes during metamorphosis. Glial cells immediately adjacent to the axons typically contain densely packed microtubules, and several layers of their processes separate each of the axons from its neighbors (Figs 1A and 2A). By the first day of pupation, however, most of these glial processes withdraw from between the axons and those remaining have lost their microtubules (Figs 1B and 2B). Some axons come to lie next to each other, and both axons and glial cells sometimes appear to be connected to each other *via* tight junctions. The outer layer of perineurial cells, which surrounds the core of

Fig. 1. (A) Cross section of the nerve supplying the mesothoracic dorsal longitudinal muscles, nerve IIN1b, from a fifth-instar larva. The nerve contains 11 large axons at this point, two having separated to innervate other muscles shortly following the bifurcation separating IIN1c, which is largely sensory, from the main trunk. The motor axons (*a*) in the main part of the nerve are all well separated from each other by glia. The collar region outside the basal lamina investing the main nerve contains numerous tracheoles (*t*), plus glia and neurosecretory axons not discernible at this magnification. 2750×. (B) Cross section of the same nerve at approximately the same point but from a 12 h pupa. The motor axons are no longer well separated by glial layers, and there are large spaces between some of them. Large phagocytic hemocytes (*gr*, granulocytes) have invaded the basal lamina around the nerve. The other cellular constituents of the collar region have both increased in size and number, with the addition of some cellular profiles of unknown origin. At a gross level, the nerve takes on a broadened, flat appearance as a result of the addition of these cells (see also Fig. 2, Rheuben, 1992). 1300×.
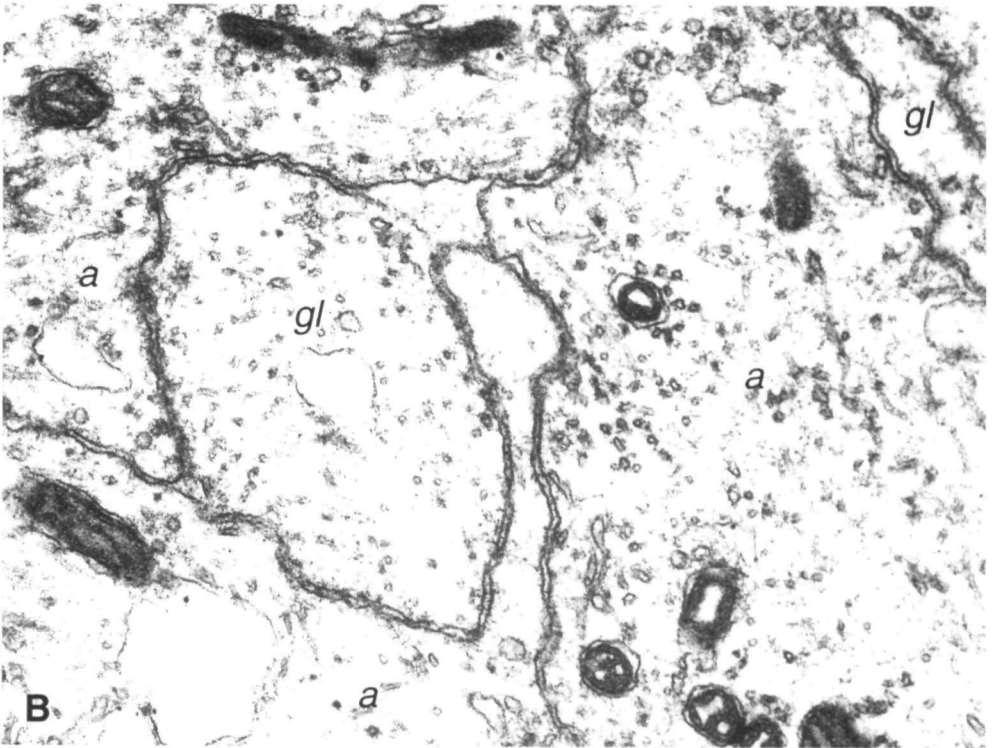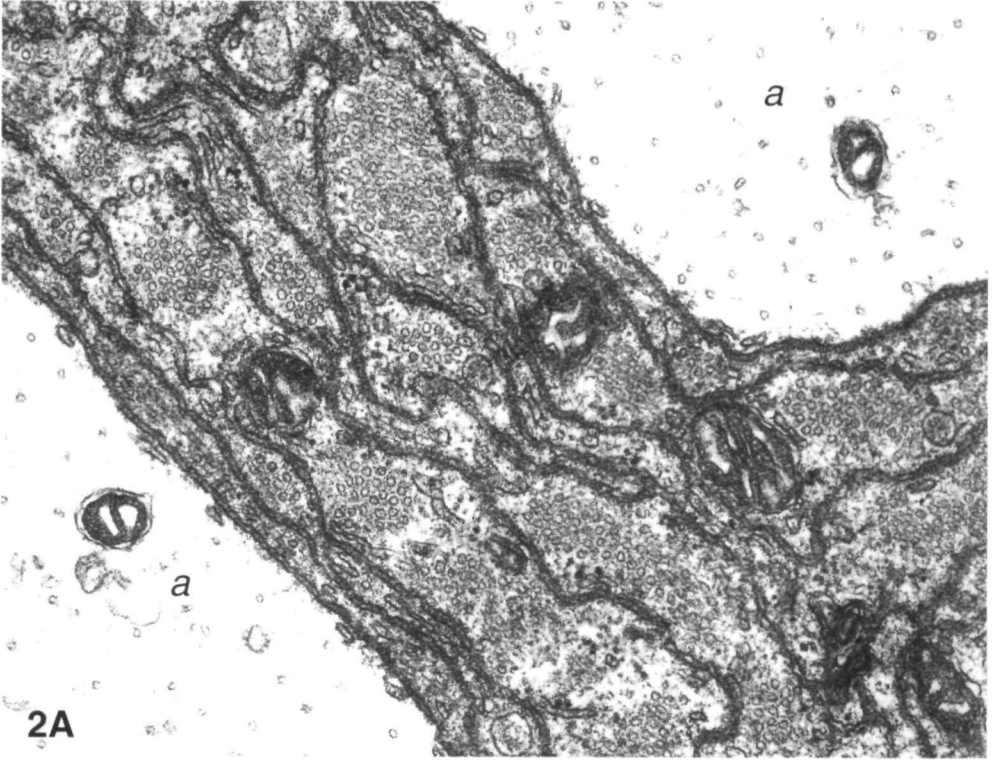
1A B
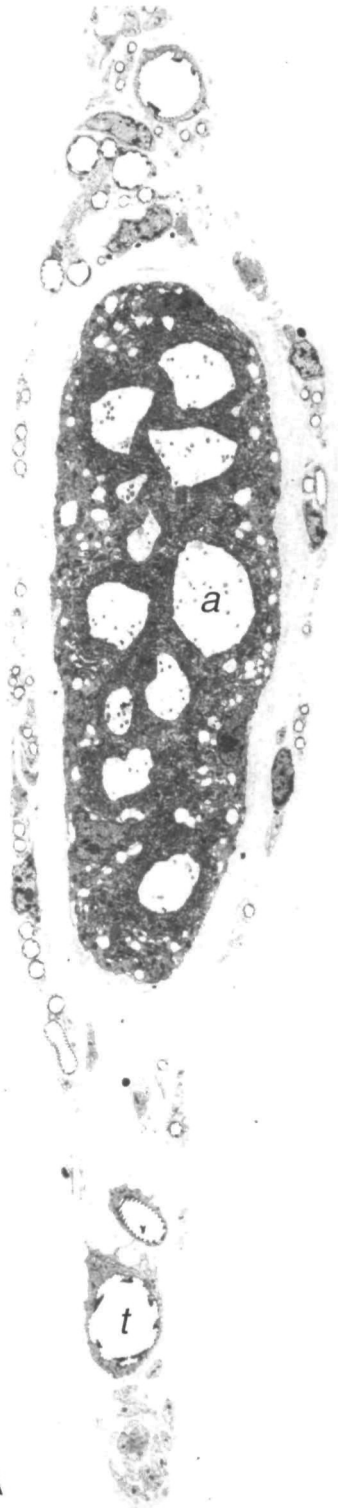
2A
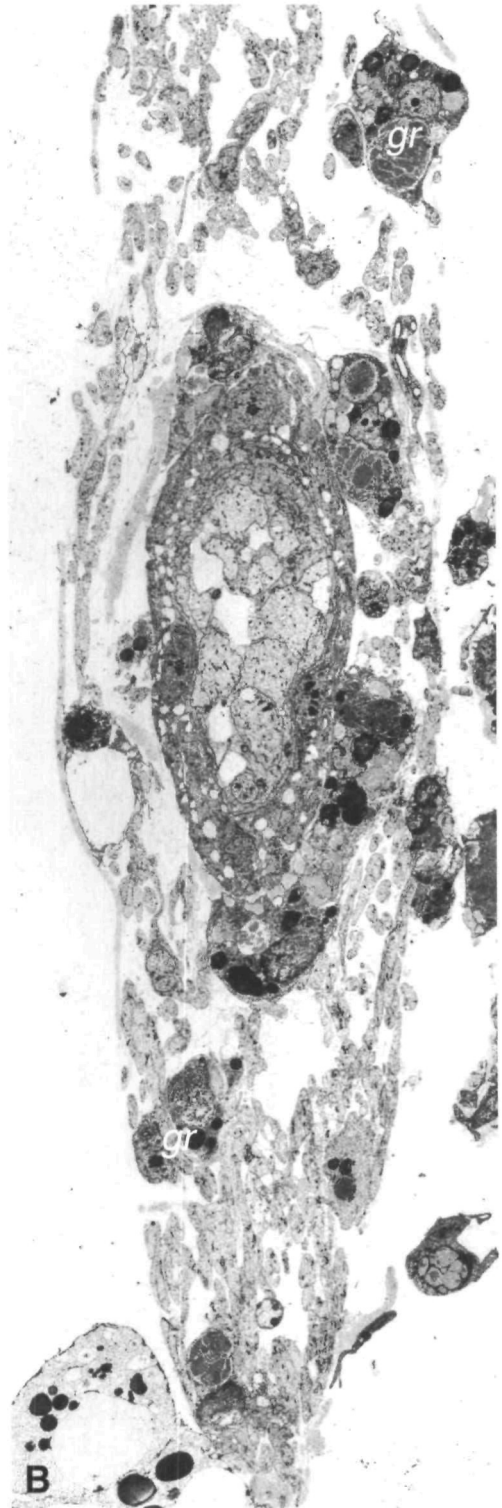
B

Fig. 2. (A) High-magnification view of the central 'core' region of nerve IIN1b from a fifth-instar larva. The portions of two axons (*a*) are separated by eight or nine layers of glial processes which are tightly packed with microtubules. 57 780×. (B) A comparable view of the central region of the nerve from a 13 h pupa. The glia (*gl*) have many fewer microtubules and become difficult to distinguish from axons (*a*) except by their overall morphology; these have been tentatively identified from low-magnification views. 47 300×.

glia and axons, appears to be more loosely organized. These changes resemble those described by McLaughlin (1974*a*) for the abdominal nerve cord, and the nomenclature used here is comparable, except that we have not categorized the perineurial cells into Types I and II since the distinctions are not clear in these peripheral nerves.

During the early stages of metamorphosis, the basal lamina in the collar region is invaded by granulocytes, which appear to be engulfing parts of it by phagocytosis (see also Rheuben, 1992). Tracheoles clump together surrounded by a single cytoplasmic envelope, and their cuticular rings appear to be deteriorating. Presumed glial processes, which typically contain microtubules, small mitochondria and rough endoplasmic reticulum, are commonly grouped into clusters of two and three profiles in the basal lamina. They are sometimes connected to each other by a septate desmosome and sometimes loosely surround a single small neurosecretory-type axon containing dense- and clear-cored vesicles of several types, similar to those described in the adult nerve to the dorsal longitudinal muscle (Wasserman, 1985). These apparent glial profiles of the collar region increase in number and appear to swell during the prepupal and pupal periods (Figs 1 and 3). Cell types whose function could not be ascertained, some of which may be myoblasts, appear in this region of the nerve trunk. This increase is most marked in the region where the nerve enters the anlagen and the collar region becomes so extensive that it appears to spread out like a triangular sheet (see Fig. 2 in Rheuben, 1992).

Changes in the secondary and tertiary muscle branches of the motor nerves

The secondary muscle branches of the motor nerves supplying the larval dorsal longitudinal muscles consist of a single fine branch of the motor axon wrapped in 2–5 layers of processes from glial cells and, frequently, a neurosecretory axon in the outermost glial loop. There appear to be two types of glial cells associated with the motor axon, with the one forming the inner wrappings having a more electron-dense cytoplasmic matrix. Some regions of the nerve have considerable extracellular space between the axon and the inner layers of glia, as shown in Fig. 4, and others do not. The appearance of these enlarged spaces could not be correlated with fixation protocol or previous stimulation history. The presumed neurosecretory axons, containing both dense-cored and clear-cored vesicles similar to those in one of the types of axons seen in the collar of the main nerve, are loosely enfolded in the outer surface of the outer (less electron-dense) glial loop of the
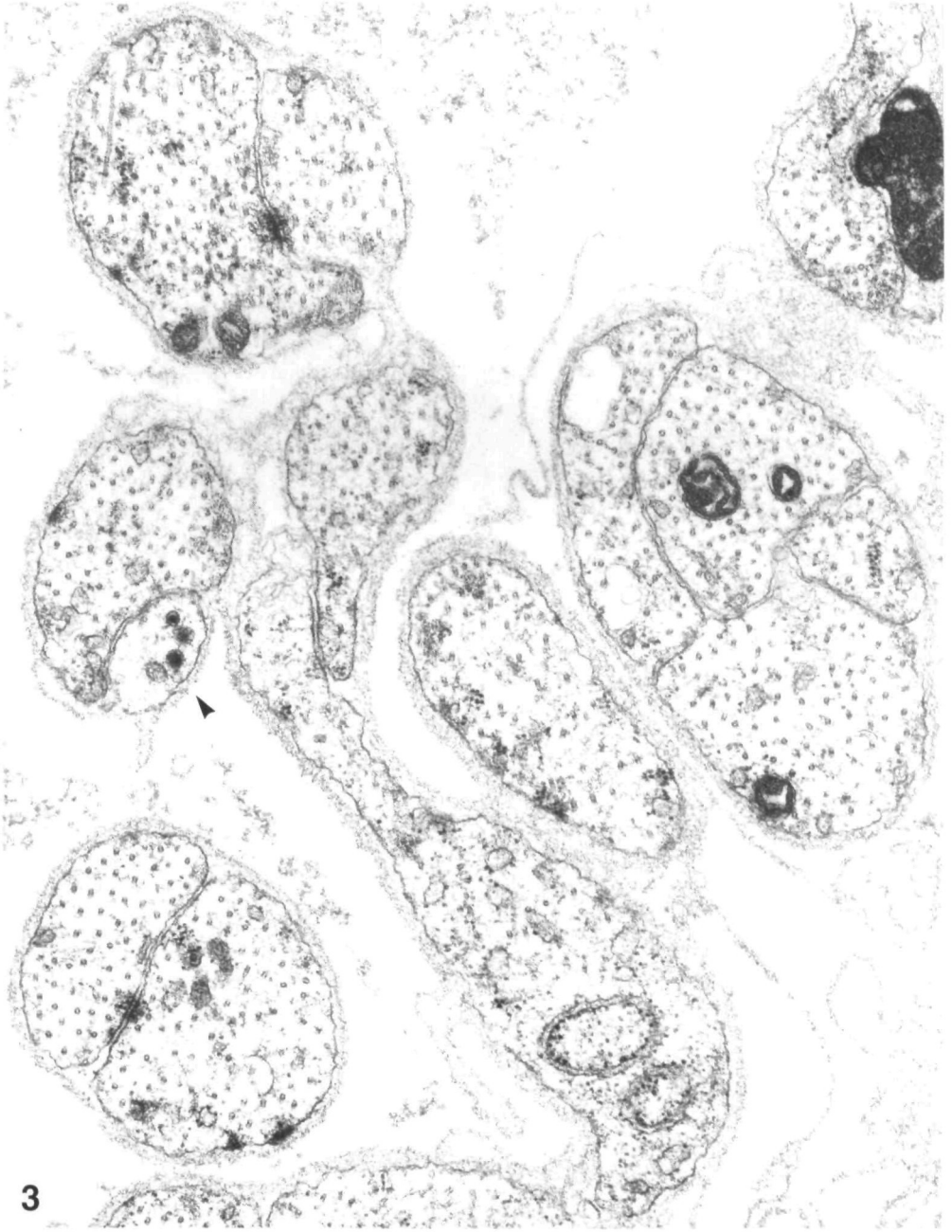
Fig. 3. Cross section through the collar region of nerve IIN1b from a 2 h pupa. In this region the de-differentiation and swelling of the various profiles is such that the identity of many cell types becomes difficult to ascertain. A neurosecretory axon (arrowhead) can be identified from its dense-cored vesicles, and presumably the cell adjacent to it is some sort of glial cell. The other closely allied profiles may also be neurosecretory twigs and their glial cells, but this cannot be ascertained without serial sections. 35 800×.

Fig. 4. Cross section of a secondary motor nerve branch to muscle AB from a fifth-instar larva. A single motor axon (*a*), two types of glial cells, judging from cytoplasmic density, and an accompanying neurosecretory axon (arrow) are shown. Muscle fiber, *m*. Compare the appearance with that shown in Fig. 5. 35 700×.

nerve branch. The neurosecretory axon is sometimes in direct contact with the hemolymph and sometimes well-wrapped by the glial cell; structural corollaries of release sites occur in swellings along the axon. Their structure will be described further in another paper (M. B. Rheuben and D. M. Autio, in preparation).

The degenerative changes in the secondary and tertiary branches of the motor nerves resemble those seen in the main nerve trunk with regard to the generalized swelling of the glial cell processes ensheathing the single motor axon and the single neurosecretory axon. Occasionally, some nerve cross sections do not appear to have an intact axon, or the axon appears somewhat shrivelled within the glial
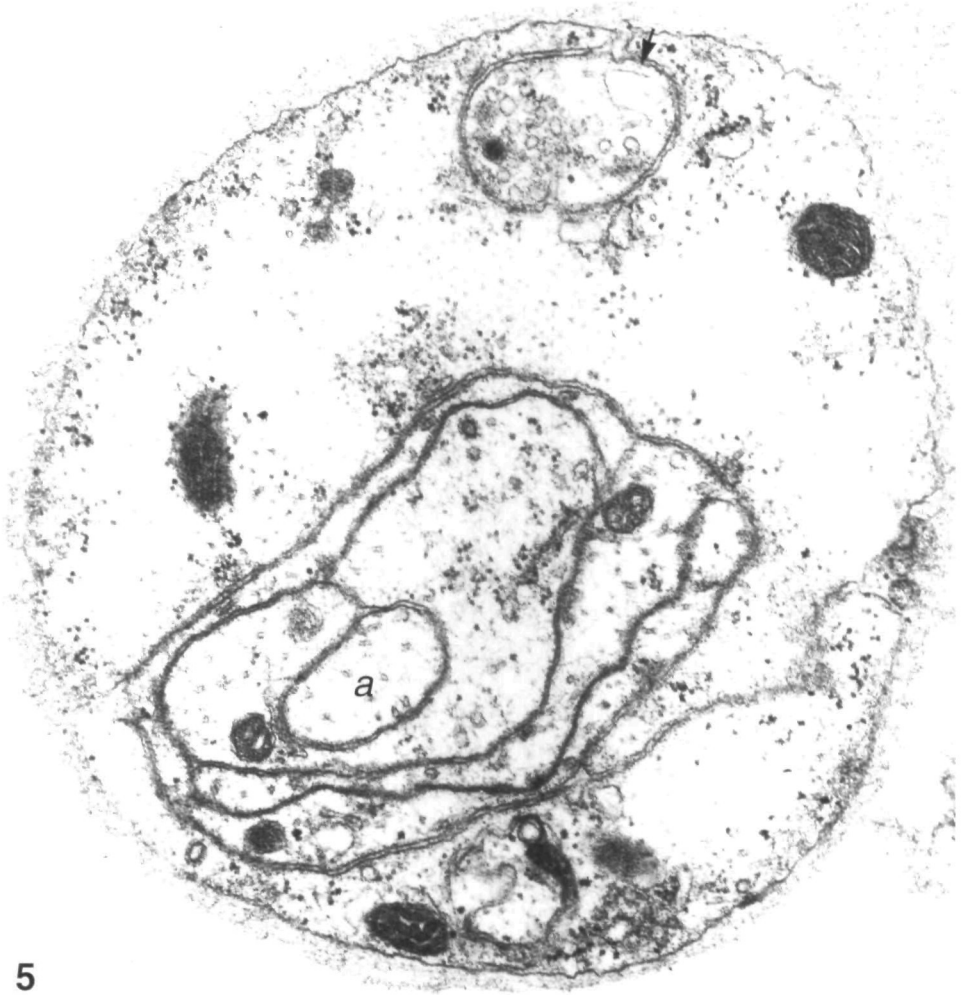
Fig. 5. Cross section of a degenerating secondary motor nerve branch to muscle AB from a 7 h pupa. Note the more electron-lucent and swollen appearance of the glial processes. Axon, *a*; neurosecretory axon, arrow. 42 150×.

folds, but most have a normal structure up to the last stage studied (12 h postecdysis). Cross sections including the neurosecretory axons are frequent (Fig. 5).

Degeneration of the neuromuscular junctions: TEM observations

The neuromuscular junctions in the larval dorsal longitudinal muscles of *Manduca sexta* have been described previously (Rheuben and Kammer, 1980; Schaner and Rheuben, 1985) and consist of a branch of the nerve terminal, 15–49 μm long, surrounded by a complex formed by interdigitating processes from both glial cells and the muscle fiber itself. Contacts between the nerve terminal and

the muscle fiber are restricted to oval regions or 'plaques', where the apposing oval patch of postsynaptic membrane contains an electron-dense thickening in TEM sections, or a dense patch of particles on the extracellular leaflet in freeze-fractured material. One or more glial processes separate each plaque from the next. The presynaptic specialization is an electron-dense bar about $0.2\,\mu$m in length corresponding to a narrow band of particles on the cytoplasmic leaflet in freeze-fractured material.

During the prepupal and early pupal period, striking morphological changes occur in the structure of the junction itself, and again it is the glia that are most noticeably affected. The glial cytoplasm is withdrawn from the fine interdigitating processes within the junction and redistributed to form one or more large bulges over its outer surface. The rather precise alternation of glial processes with muscle fiber plaques is disrupted.

Because initial examination of the prepupal and pupal mesothoracic muscles indicated that degeneration of the neuromuscular junctions was not proceeding uniformly in different muscles, and because this study was being performed in conjunction with physiological studies, we developed a method of staging the sampled regions of the junctions, as seen in thin sections, in order to have some quantitative assessment of the structural changes to relate to the physiological measurements.

Stage 0 (Fig. 6A) is defined as the normal fifth-instar neuromuscular junction before the beginning of the metamorphic change, as described above. Besides the profile of the nerve terminal, the dominant feature of the junction is the complex of muscle and glial processes. Within this complex the ratio of glial processes to muscle fiber processes is approximately 40 % glia to 60 % muscle. Wherever the nerve terminal is in direct contact with the muscle fiber process, the muscle membrane is specialized into oval plaques, appearing stiffened and electron-dense with small protuberances into the synaptic cleft, similar to those found in the adult (Rheuben and Reese, 1978). Glial processes are apposed to the terminal around the remainder of its circumference. Clusters of clear vesicles are found within the nerve terminal cytoplasm near the active zones. One or more tracheoles and tracheoblasts run parallel to the long axis of the junction along its sides. The contours of the junction blend smoothly with the outline of the surface of the muscle fiber.

Stage 1 denotes an early stage of degeneration (Fig. 6B). All of the elements of the stage 0 junction are present, but the relative proportions are different. The glial cell process covering the outer surface of the junction is rounded up, usually with bulges on either side of the junction ('dumbell shape' in cross section), instead of being very thinly and evenly draped. Glial fingers of normal appearance are still intertwined with the muscle cell processes, but the proportions are decreased to about 30 % glia to 70 % muscle. The nerve terminal looks normal, with synaptic vesicles, active zones and postsynaptic densities. The profile of the junction protrudes above the contours of the muscle fiber, which is itself shrivelling.

At stage 2 there is clear evidence for further withdrawal of glial processes from
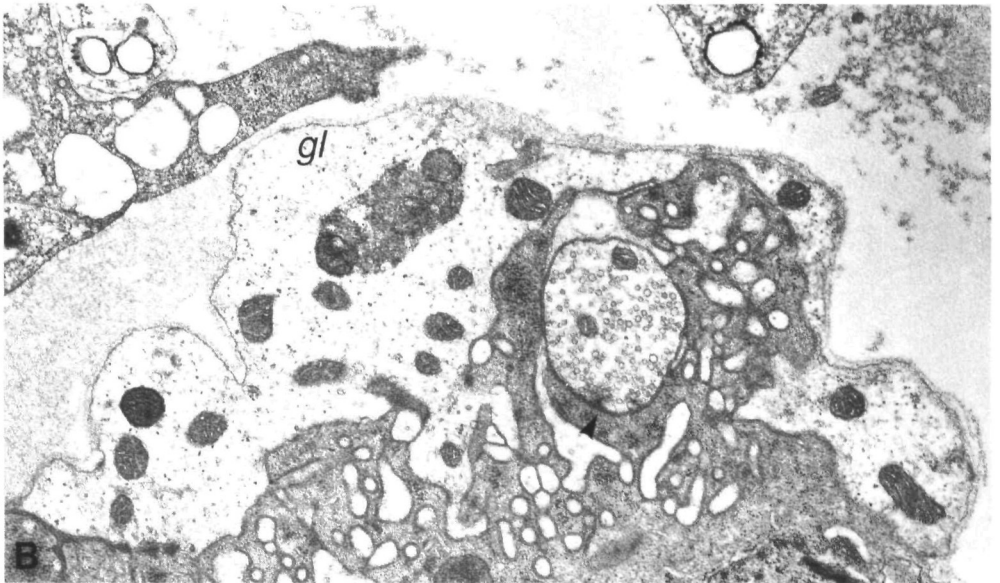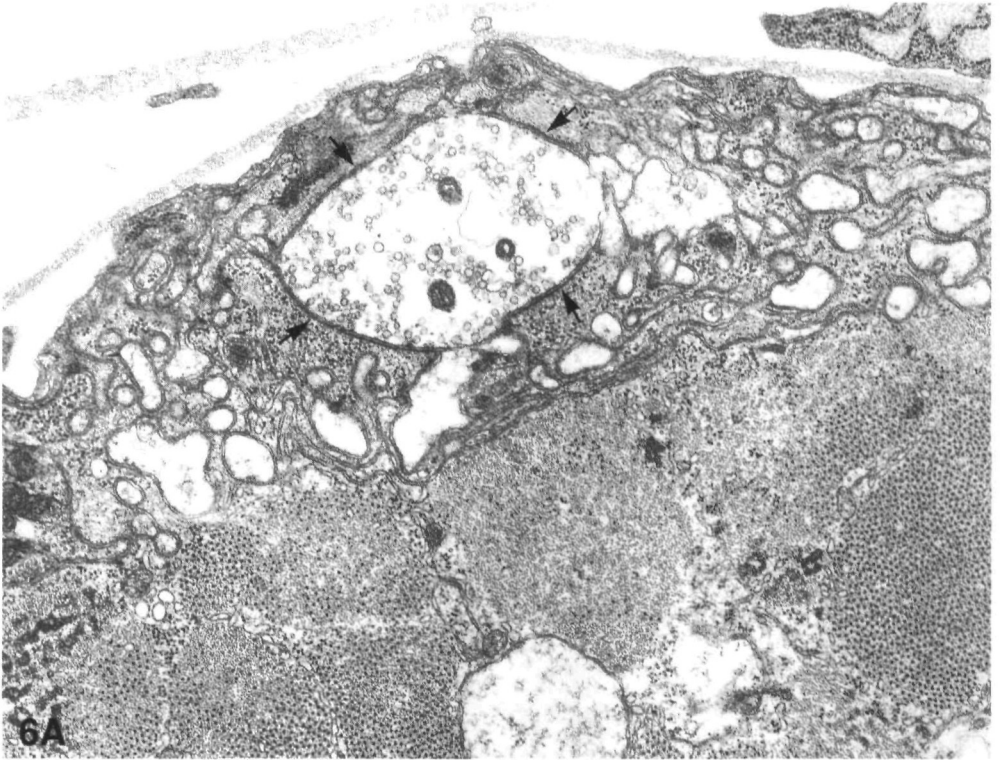
the interstices between muscle fiber processes: unfilled extracellular spaces are found within the junction, profiles of glial processes lie next to each other, and muscle processes are collapsed on one another. The nerve terminal still looks functional, with synaptic vesicles in normal numbers, and pre- and postsynaptic

Fig. 6. (A) Stage 0, normal neuromuscular junction from an AB fiber of a fifth-instar larva. The nerve terminal is in contact with processes from the muscle fiber in four separate locations (arrows); the postsynaptic membrane is increased in electron density. The glial processes are electron-lucent and are predominantly within the junction. The layer covering the outer surface of the junction is very thin. 23 350×. (B) A stage 1 junction from an AB fiber of 7.5 h pupa. The nerve terminal is still maintaining some normal contacts with the muscle; one here contains a presynaptic dense body (arrowhead). The glial cell cytoplasm (*gl*) forming the outer layer of the junction makes up a much larger proportion of the total. 17 450×.

specializations of normal appearance. There is further build-up of glial cytoplasm on the sides of the outer surface of the junction (Fig. 7A).

In stage 3 junctional profiles (Fig. 7B) nearly all of the processes from the glial cell are withdrawn, leaving empty extracellular spaces within the junction or regions in which the muscle processes have consolidated and collapsed on one another. The proportion of glial cytoplasm mounded up at the sides of the junction is greater than the volume occupied by muscle processes, glial processes and the nerve terminal combined. The nerve terminal itself may change its relationship to the remaining muscle, either becoming completely surrounded by muscle processes (see Fig. 9) or by appearing to migrate out of the junction, coming to sit isolated on the surface of the muscle fiber, largely surrounded by a large swollen glial process. The junction as a whole is smaller, and in some cases is only connected to the rest of the muscle fiber by one or more thin stalks of muscle cytoplasm (see Fig. 10). In junctions categorized as stage 3 or earlier, the nerve terminal continues to look potentially functional, with intact membrane, synaptic vesicles and at least one set of pre- and postsynaptic specializations of normal appearance. Structures looking like coated vesicles (see below) may be seen loose in the extracellular spaces adjacent to and within the junction starting with stage 3.

At stage 4 (Fig. 8A) the glial cell may or may not have the dumbbell shape seen in previous stages, and it often appears to be completely removed from the junction. The nerve terminal no longer looks functional: either there is no contact with the muscle, the terminal being entirely surrounded by glial cell processes (see Fig. 12) or its membranes being disrupted, or there is no identifiable nerve profile present. Occasionally abnormal nerve profiles are seen completely surrounded by muscle (Fig. 11). Tubular invaginations in the muscle, appearing in sections as round holes, may contain remnants of membranes or be empty.

In stage 5 junctional regions, the glial cell may be totally detached from the junction, and only one or two of the components of a typical junction can still be recognized (Fig. 8B). Often there are only a few invaginations into the muscle, some containing structures like coated vesicles. Intact (with the surrounding membrane complete) sections of the nerve terminal are no longer to be found within the junctions. Remaining nerve structures are engulfed or encircled by the associated glial cell; it is not clear whether this process represents phagocytosis or protection (compare Fig. 7B and Fig. 12).

In some degenerating junctions large numbers of structures looking like coated
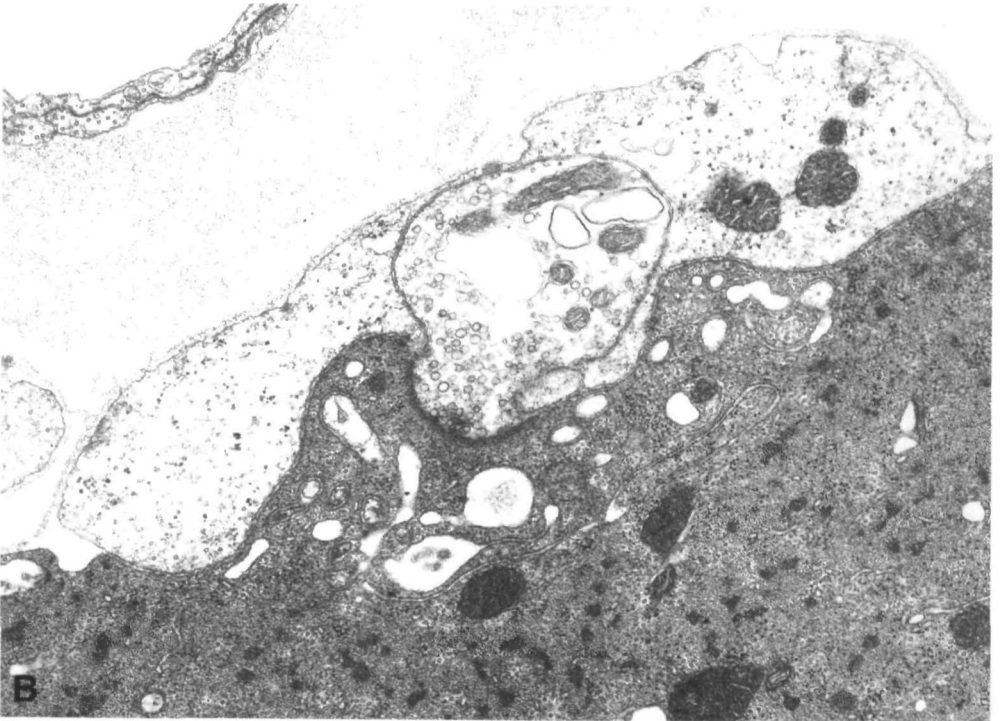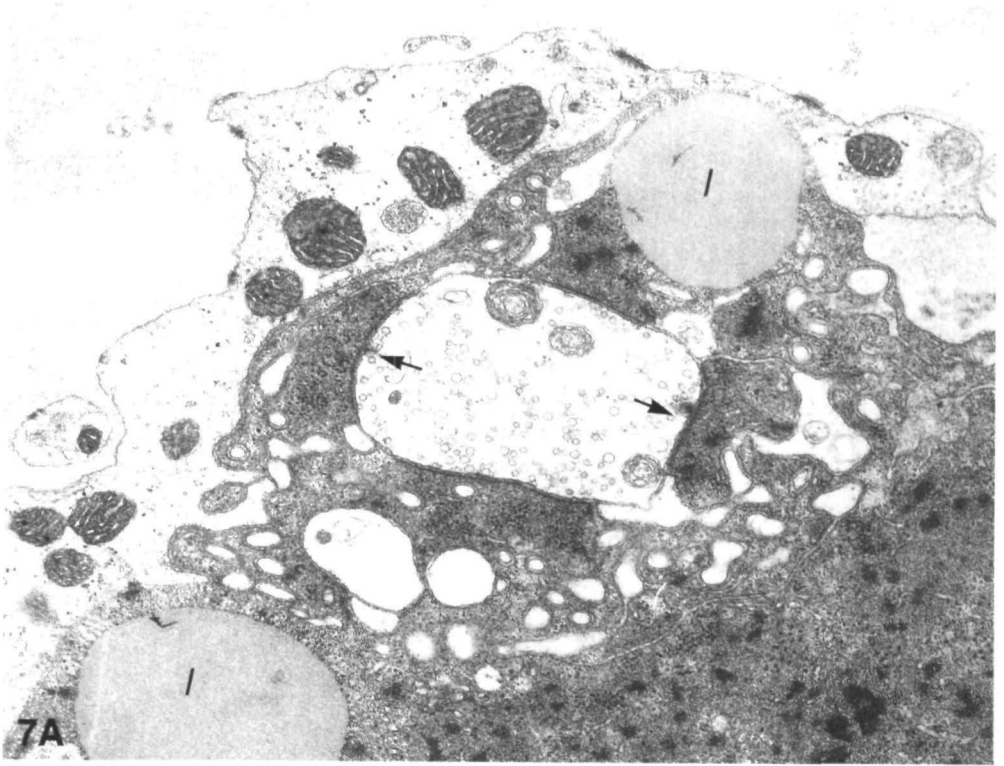
Fig. 7. (A) Stage 2 degenerating junction from an AB fiber of a 2h pupa. Normal contacts with the muscle fiber are still made by the nerve terminal; here four are present, two with presynaptic dense bars (arrows). The ratio of glial processes to muscle processes in the complex around the nerve terminal is decreased compared to stage 1. Two liposome granules are present (*l*). 23 850×. (B) Stage 3 degenerating junction from a C fiber of a 2h pupa. Almost all glial processes have been withdrawn from the junction, leaving muscle processes collapsed on each other and a few empty holes. The nerve terminal continues to make a potentially functional contact with the muscle fiber, with both pre- and postsynaptic specializations, but is otherwise almost entirely surrounded by the glial cell. 23 850×.

vesicles are found in the extracellular spaces. These spherical structures are, on average, 64.8 nm in diameter, including the outer fuzzy layer. Fig. 11 illustrates a junction in which similar structures are found both within the nerve terminal and in the extracellular space adjacent to it. If these structures are not artifactual, their occurrence in the extracellular space may indicate that some terminals rupture during degeneration. Beaulaton and Lockshin (1978) attribute smaller (30–60 nm), unlayered spherical structures in the extracellular space of the degenerating junctions of *Antheraea polyphemus* and *Manduca sexta* to breakdown of the subsynaptic reticulum.

In order to answer some questions regarding the rates and the uniformity of the various degenerative processes, muscles were sampled extensively at different times during the first day after pupal ecdysis. Fibers were sectioned primarily in the regions from which electrophysiological recordings (Sonea and Rheuben, 1992) were obtained, as indicated in Fig. 1 of Rheuben (1992). Pupal AB fibers were sectioned largely in the caudal portion of the muscle (32 block faces, from 15 animals), with seven levels sectioned in the rostral region and three in the central region. C fibers were sectioned in the rostral ventral one-third of the muscle (20 block faces from nine animals) with nine block faces from the caudal dorsal end of the muscle (as generally outlined on Fig. 1 of Rheuben, 1992). Little sectioning was done in the region of the developing anlagen, close to the center of the muscles, and the time course of changes in nerve and muscle in that area might well be different from that described below.

Previous work (Randall and Pipa, 1969) on the larval proleg retractor muscle in *Galleria mellonella* indicated that the rate of degeneration of the neuromuscular junctions was faster at the cuticular ends of the muscle fibers. Further, the time at which degeneration begins for individual muscles is quite different, with some degenerating at the end of the fifth instar, some early in the pupal period, and others not degenerating until after the end of the pupal period (see Weeks and Truman, 1984, for examples). Consequently, we examined several of the dorsal longitudinal muscles for corresponding differences in time courses that could be correlated with the physiological studies.

In *Manduca* larvae, each of the mesothoracic dorsal longitudinal muscles has a relatively small number of very large muscle fibers, so individual muscle fibers from day 1 pupae were identified in thick sections and within the blocks. Each of
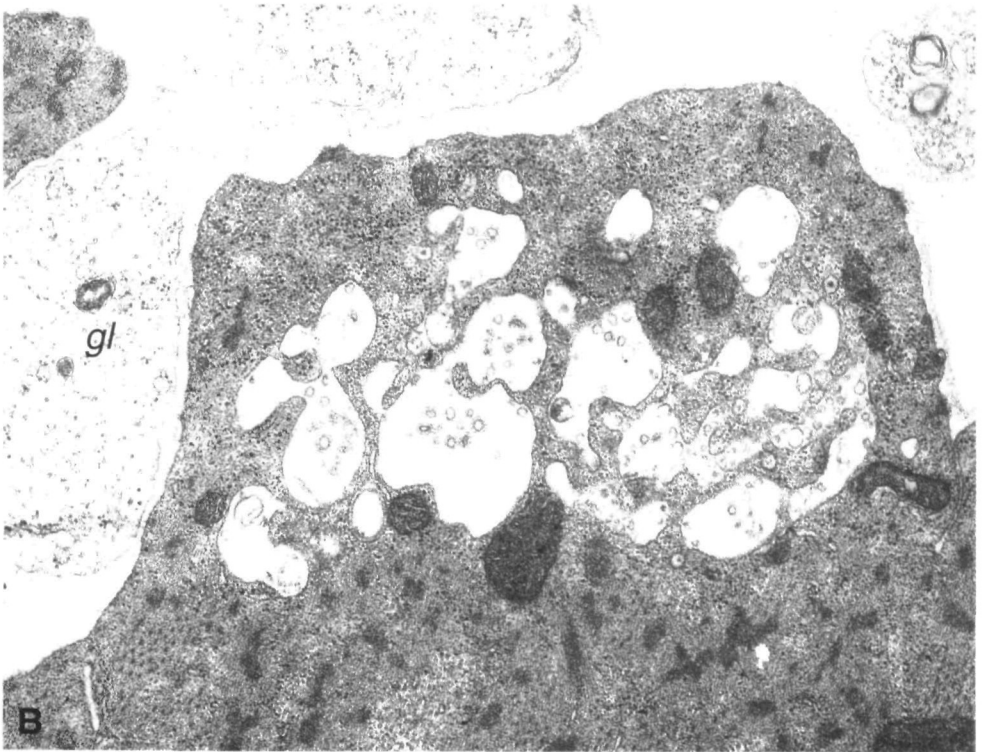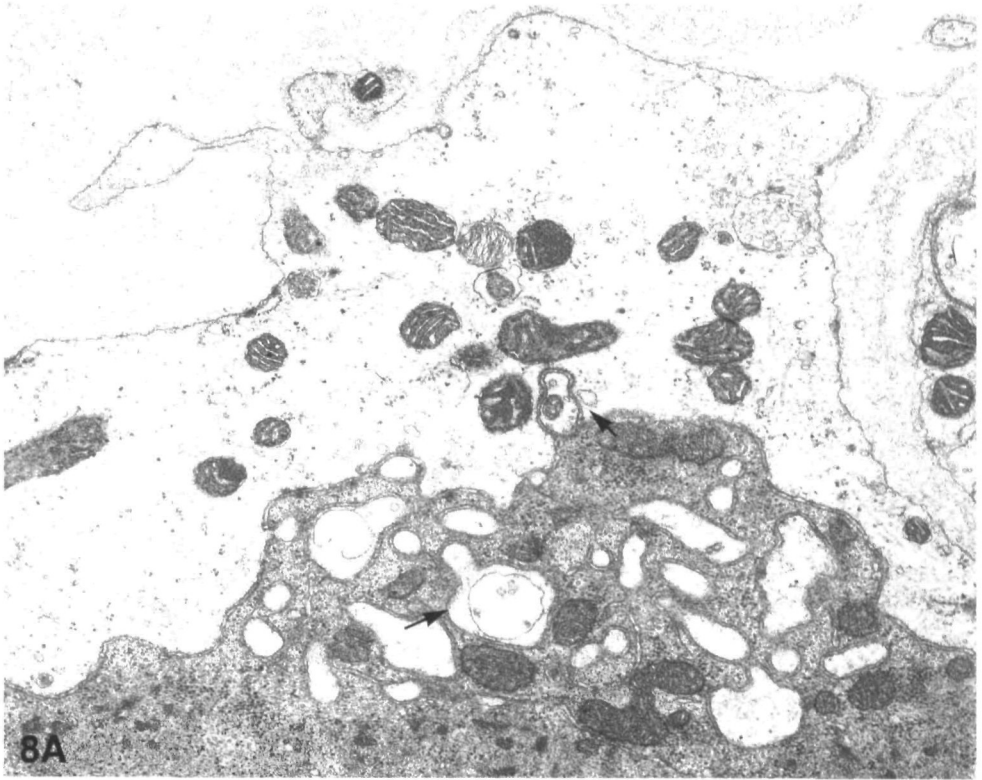
Fig. 8. (A) Stage 4 degenerating junction from a C fiber of a 1 h pupa. In this region of this junction, no apparently functional contacts between nerve and muscle can be identified. Arrows indicate what may be remnants of the nerve terminal. Most of the bulk of the glial cell lies outside the junction. 23 850×. (B) Stage 5 degenerating junction from a C fiber of a 2 h pupa. All the glial processes have withdrawn from the junction, and no profiles of the nerve terminal can be identified. The glial cell (*gl*) is nearby. Small structures looking like loose-coated vesicles are seen in the holes in what is left of the junctional complex. 20 900×.
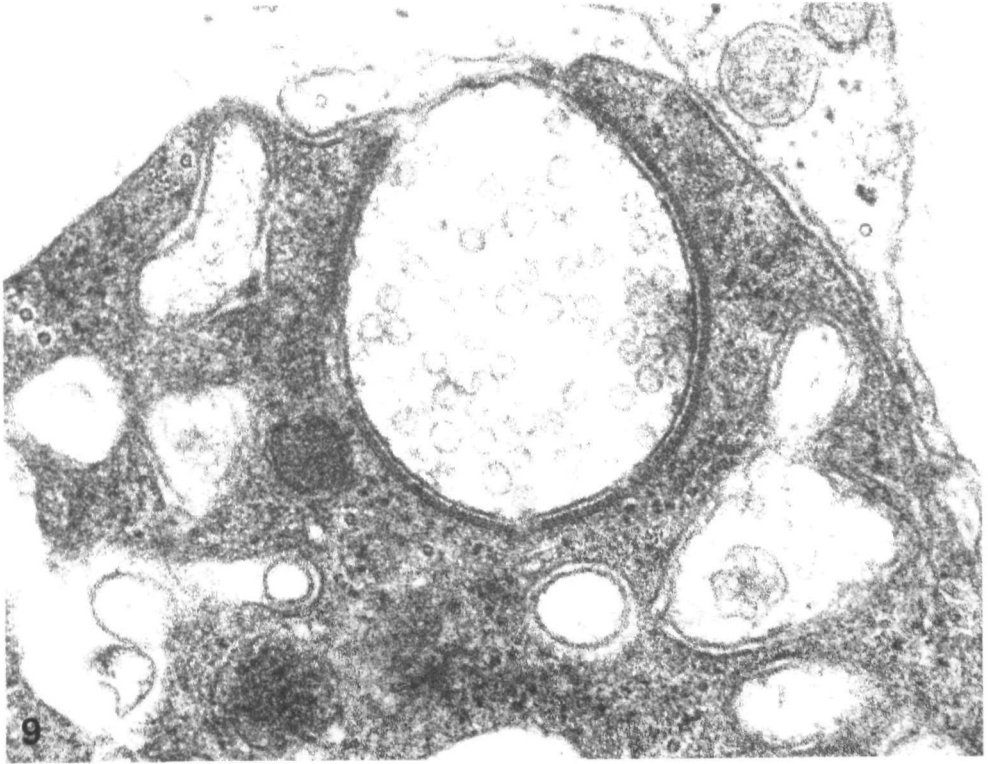

Fig. 9. Nerve terminal from a C fiber of a 4 h pupa. Almost the entire circumference of the nerve terminal is in apposition to specialized electron-dense postsynaptic membrane. 78 900×.

their junctions was photographed and mapped and its stage of degeneration was determined from thin sections. The stages were color-coded and plotted on a diagram of the muscles at the level at which the block was sectioned. No trends could be detected. The junctions at the extreme ends of the fibers did not appear to be degenerating faster or slower than those one-third to three-quarters of the way to the middle.

In 10 animals the same block was sectioned at two or more levels, each separated by at least a millimeter. The mean stage score for the level closest to the
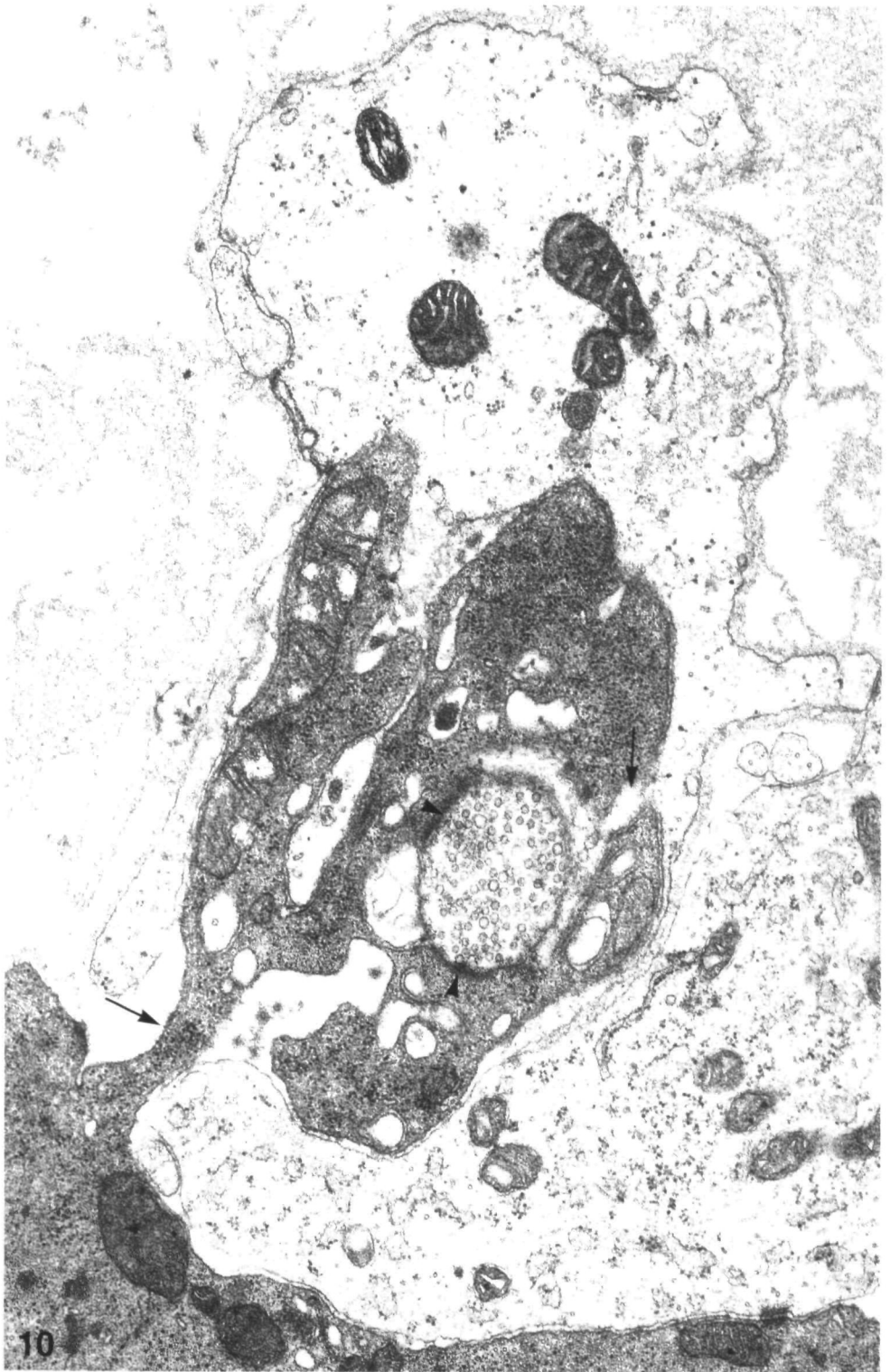
Fig. 10. Neuromuscular junction from a C fiber of a 1 h pupa. In this region of the terminal, the junction is connected to the main part of the muscle fiber by only a thin stalk (arrow). The nerve terminal makes contact with the muscle fiber processes in two places, which appear to have postsynaptic specializations (arrowheads). The glial cell has withdrawn most of its processes from the junction. 29 800×.
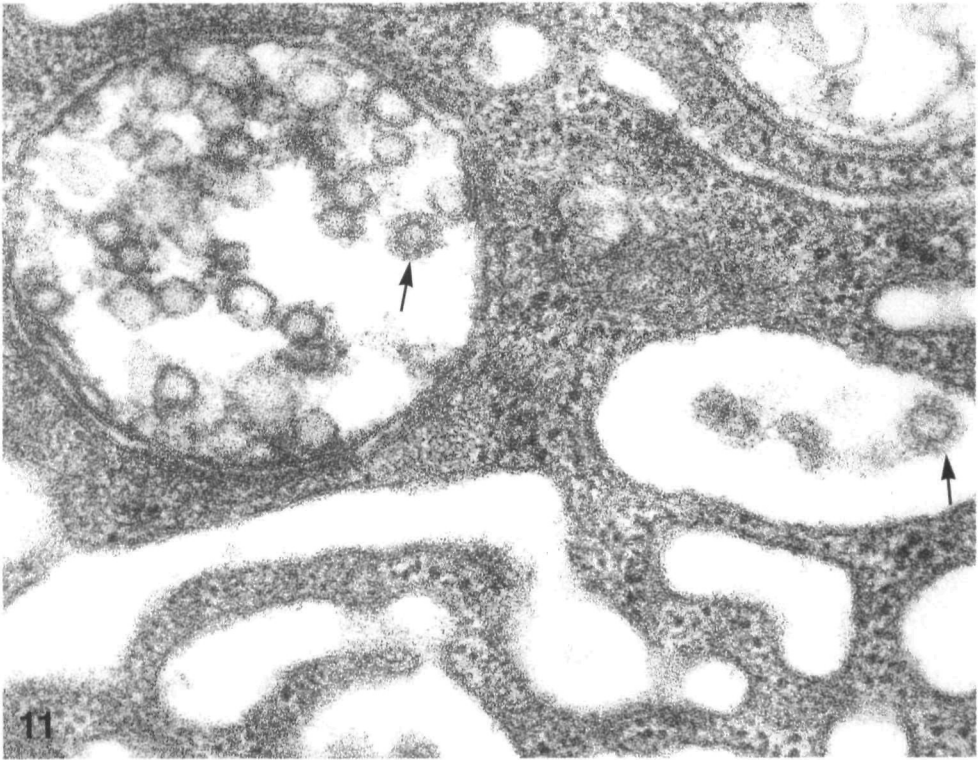
Fig. 11. Nerve terminal from a C fiber of 2 h pupa. The glial processes have entirely withdrawn, and the nerve terminal is completely surrounded by muscle fiber, essentially all of which exhibits the appearance of specialized postsynaptic membrane. Both the nerve terminal and the adjacent empty spaces contain structures looking like coated vesicles (arrows). 115 200×.

end of the fiber was compared to those obtained from the more central levels. Five animals had an increase in stage score from the cuticular end towards the middle and five did not. This indicates that, over the region sampled, there was no gradient of degeneration along the lengths of the fibers.

There also did not appear to be any correlation between stage of degeneration of individual junctions and the particular muscle fiber on which they were found. If an individual muscle fiber was examined at two or more levels, with the separation of the levels being greater than the average junctional length, the stages of the
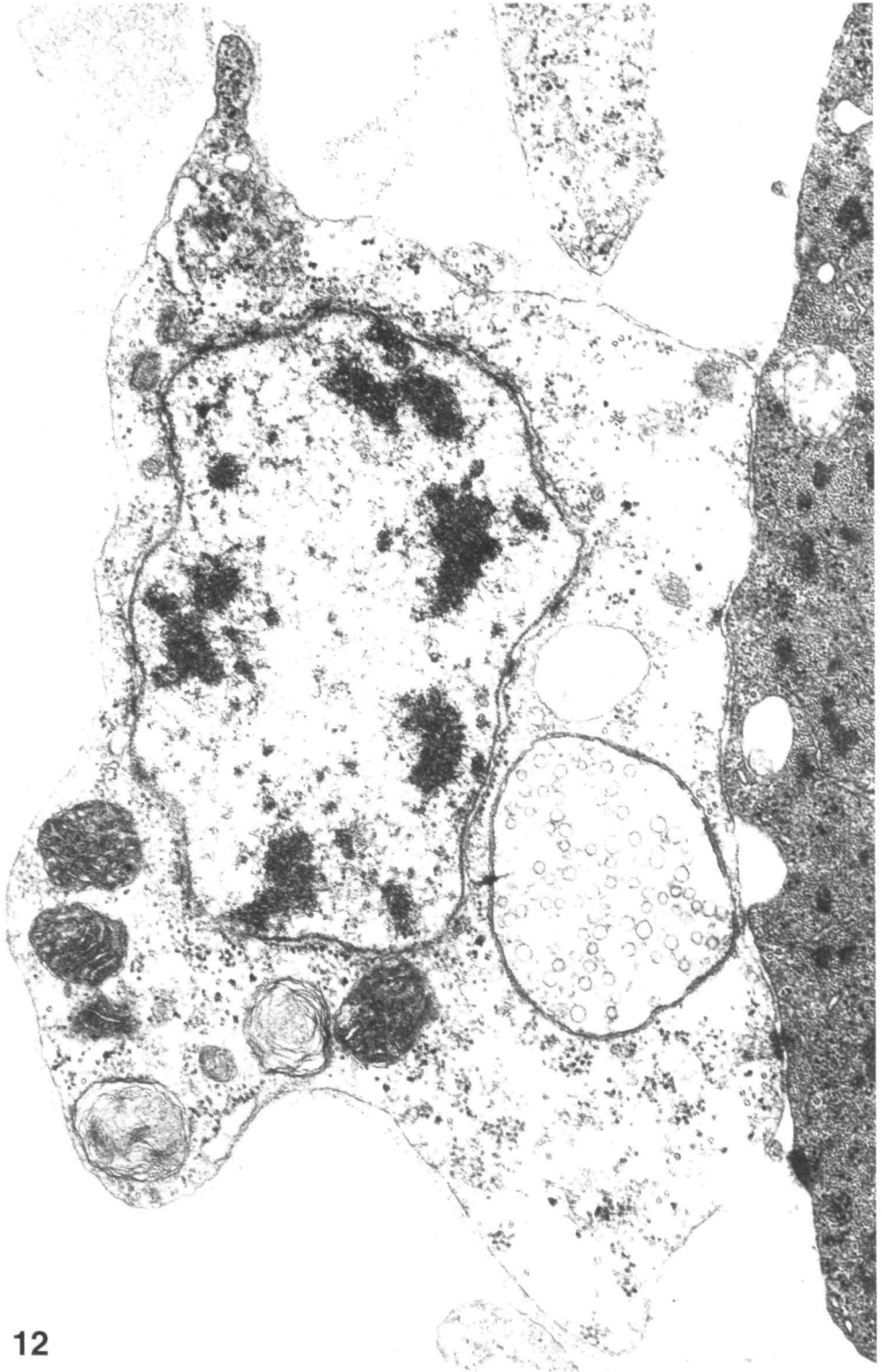
12

Fig. 12. Nerve terminal from a C fiber of a 2 h pupa (same animal as Fig. 11). In this junction, the nerve terminal has been completely surrounded by the glial cell. 42 900×.

profiles obtained from those junctions also varied. The average difference in stage scores of junctions from the same fiber at different levels was compared to the average differences in scores between junctions on different fibers at the same level in seven animals. The average difference was 0.77 ± 0.67 ($N=22$) stage points for junctions on the same fiber and 0.91 ± 0.81 ($N=39$) for junctions at the same sectioning level but on different fibers. While there appears to be somewhat less variability among junctions on the same fiber, the difference in both cases is less than 1 stage point and less than the degree to which we can accurately stage the junctions. So, as far as we are able to determine, the junctions on individual muscle fibers are degenerating at similar rates within a given muscle.

To examine the variability of the degree of degeneration within a single junction, two blocks from animals 4–6 h post-ecdysis were sectioned at three consecutive levels $10 \mu m$ apart. Since the average junctional length has been previously determined (Schaner and Rheuben, 1985) to range from 15 to $49 \mu m$, many junctions would be sampled two or more times, and this spacing would cover a reasonable proportion of the length of a junctional branch. All junctions and fibers in the block faces were identified and photographed. Thirteen junctions from a C muscle block and nine junctions from an AB block were examined and stage numbers were assigned blindly by two observers. At this spacing, the profiles from a particular neuromuscular junction appeared more like each other than profiles from different junctions. Nevertheless, junctional scores varied by 1–2 stages at the three levels. It was apparent from comparing the scores of the two observers that the difference between stage 2 and stage 3 or stage 4 and stage 5 was occasionally ambiguous or subjective, but that the difference between stage 3 (functional intact nerve terminal, postsynaptic specialization intact) and stage 4 (non-functional appearance, nerve terminal membrane disrupted or not in contact with a muscle process) could be consistently determined. Consequently, the data were examined with regard to this distinction.

Of 19 junctions that were identified and sectioned at two or more levels, three appeared 'functional' at all levels, 13 exhibited profiles appearing functional at some levels and non-functional at others, and three appeared non-functional at all levels. The differences within a junction at $10 \mu m$ intervals were not so great as to reveal any dramatic trends. In 15 junctions present at all three levels, 11 had scores that varied in a consistent fashion, either two adjacent the same followed by one higher or lower (e.g. 3, 3, 4 or 3, 3, 2) or a steadily increasing series, but four had stage scores that were not in sequence (e.g. 3, 5, 2). This distribution is not different from what would be expected by chance, so we cannot say with any certainty that the junctions degenerate from the tip back towards the region where the motor axon first contacts the muscle, although that might be the case. When all profiles were included, 35 % of those from the AB block were non-functional and 52 % of those from the C block were non-functional, which is comparable with the

Table 1. *Distribution of degeneration scores as a percentage of the total*

| | Degeneration stage score | | | | |
Age	1	2	3	4	5
AB fibers					
0–3 h	16 %	38 %	28 %	13 %	5 %
	(10)	(23)	(17)	(8)	(3)
4–6 h	13 %	24 %	24 %	29 %	9 %
	(6)	(11)	(11)	(13)	(4)
7–9 h	14 %	42 %	16 %	19 %	9 %
	(6)	(18)	(7)	(8)	(4)
12–13 h	0 %	7 %	7 %	57 %	29 %
	(0)	(1)	(1)	(8)	(4)
Totals, 0–13 h	13.5 %	32.5 %	22.1 %	22.7 %	9.2 %
	(22)	(53)	(36)	(37)	(15)
C fibers					
0–3 h	9 %	18 %	30 %	21 %	21 %
	(3)	(6)	(10)	(7)	(7)
4–6 h	4 %	20 %	30 %	30 %	16 %
	(3)	(17)	(25)	(25)	(13)
7–9 h	6 %	10 %	45 %	26 %	13 %
	(2)	(3)	(14)	(8)	(4)
12–13 h	0 %	0 %	13 %	40 %	47 %
	(0)	(0)	(2)	(6)	(7)
Totals, 0–13 h	4.9 %	16 %	31.4 %	28.4 %	19.1 %
	(8)	(26)	(51)	(46)	(31)

Parentheses indicate the actual numbers of junctional profiles having that score.

proportions obtained from the entire population of junctions sampled (see below, Table 1).

Table 1 presents the distribution of stages in the regions of AB and C muscles examined. No completely normal (stage 0) junctions were found in muscles from pupae within the first 13 h after ecdysis. There appeared to be a marked increase in the proportion of the later stages (4 and 5) in the junctions from older (12–13 h) pupae in both muscles, although the sample from this age bracket is smaller. When stage scores for all profiles were totalled, 31.9 % of the junctions sampled on AB fibers appeared to be non-functional (stages 4 and 5) whereas 47.5 % of those on C fibers appeared to be non-functional (all fibers, 0–13 h). The distribution of stages in the two muscles is plotted in Fig. 13, and indicates a slight tendency for the junctions on C fibers to degenerate faster than those on AB fibers.

The different stages of degeneration were characterized by the degree to which the glial cell processes changed their relationship both with the nerve terminal and with the processes from the muscle fiber. The glial cells of insects have been shown to be important to neuromuscular transmission by taking up glutamate from the synaptic region (Faeder and Salpeter, 1970; Salpeter and Faeder, 1971; Botham
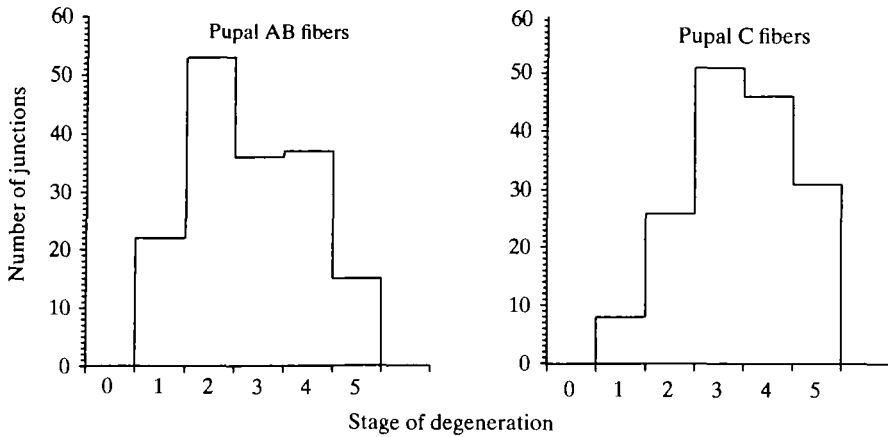
Fig. 13. Distribution of stages in AB fibers and C fibers from pupae 0–13 h after ecdysis. 163 AB junctions and 162 C junctions were staged. There appears to be a slightly greater preponderance of the more degenerated stages on C fibers compared to AB fibers.

et al. 1979), and they define structurally the borders around the postsynaptic specialization. Several of the thin-section images indicated a striking increase in length of some of the postsynaptic membranes juxtaposed to the nerve (Figs 9 and 11), which might have resulted from the withdrawal of the glial processes. The size and area of postsynaptic membrane would be expected to affect the amplitude and time course of the synaptic currents directly. We therefore examined quantitatively the effects of glial withdrawal from the junction on the relationship of the remaining muscle processes with the nerve terminal.

In fifth-instar larval muscles and pupal muscles from animals 0–8 h after ecdysis, the lengths of the regions of contact between nerve terminal and muscle process were measured from transmission electron micrographs at 65 750×. A continuous region of contact was defined as any uninterrupted contact between a muscle process and the nerve terminal, regardless of whether the boundaries of the electron-dense postsynaptic specialization could be clearly defined in that particular section. Only cross sections of the nerve terminal where its profile was circular were used to determine terminal circumferences.

The individual lengths of regions of continuous muscle contact for larval and pupal AB and C nerve terminals were compiled into histograms (Fig. 14); the means are given in Table 2. The mean diameter of normal larval postsynaptic plaques measured from freeze-fracture images where the entire plaque could be seen was 0.87 µm (Schaner and Rheuben, 1985), so these averages from TEM images, which include the shorter grazing sections through the edges of plaques, are comparable, with an average of 0.6 µm. If larval and pupal muscles are compared, both the histograms and the averages indicate an increased frequency of very long contact lengths in the degenerating junctions. There is very little change in the average circumference of the nerve terminals between larvae and
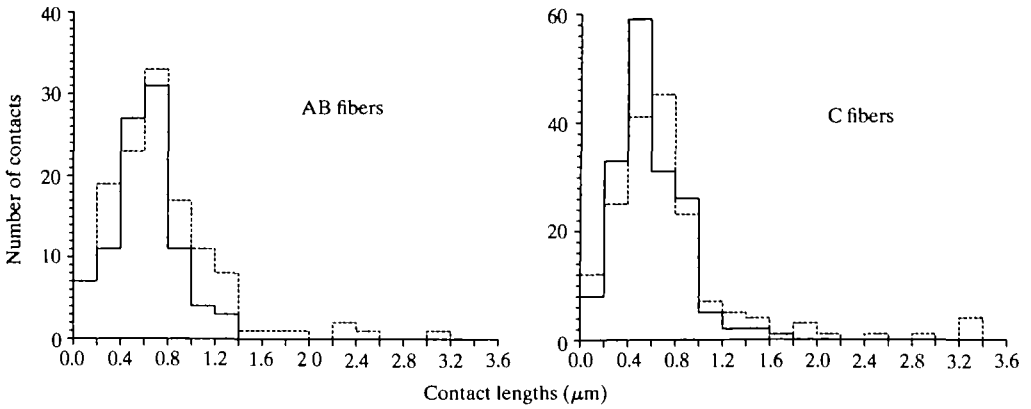
Fig. 14. Distributions of lengths of contact of nerve terminal with muscle processes of AB and C fibers. The solid lines are contact lengths from normal fifth-instar fibers and the dotted lines are contact lengths from pupal fibers 0–8 h old. There is an increase in the number of very long contact lengths in pupal fibers. The total number in each sample was 94 from normal AB fibers, 125 from pupal AB fibers, 167 from normal C fibers and 172 from pupal C fibers.

Table 2. *Average lengths of continuous contact with muscle processes*

Larval AB	$0.61 \pm 0.27 \mu$m, $N=94$
Pupal AB	$0.74 \pm 0.48 \mu$m, $N=125^*$
Larval C	$0.58 \pm 0.28 \mu$m, $N=167$
Pupal C	$0.78 \pm 0.83 \mu$m, $N=172^*$

* Significantly different from the larval values, $P<0.05$.

Table 3. *Contact length as a percentage of nerve terminal circumference*

Larval AB	$47.8 \pm 18.5\%$, $N=26$
Pupal AB	$57.4 \pm 23.1\%$, $N=41$
Larval C	$38.8 \pm 21.0\%$, $N=48$
Pupal C	$48.8 \pm 26.7\%$, $N=68$

pupae, (larval AB, 3.15μm; pupal AB, 3.02μm; larval C, 3.19μm; pupal C, 3.82μm) even though the contact lengths, expressed as a percentage of the nerve terminal circumference (Table 3), increased in the degenerating fibers. This indicates that the increases in contact lengths were probably not associated with a swelling of the nerve terminal but rather with a replacement of glial processes by muscle processes next to the membrane.

In degenerating muscle fibers, the specialized postsynaptic membrane of a plaque was sometimes surrounded by a ring of unspecialized membrane, which

was also in contact with the nerve terminal. In addition, some junctions contained very long contact regions in which postsynaptic specialization was present almost continuously (Figs 9 and 11). These observations, taken together, suggest that the junctional structure is very plastic. When the glial processes withdraw, it appears as though the spaces are filled by expansions of the muscle processes and that eventually there may be addition of postsynaptic receptors to parts of these contact regions.

Freeze-fracture observations of degenerating neuromuscular junctions

Regions of fifth-instar, prepupal and pupal muscles examined in the TEM were also prepared for freeze-fracture. The appearance of a normal fifth-instar terminal is shown in Fig. 15, which was selected to illustrate the full range of appearances of the pre- and postsynaptic specializations, including some of the less common arrangements. A 'normal' presynaptic plaque consists of a flattened oval region, bordered by membrane with an increased density of small particles, and surrounding an active zone composed of a narrow band of particles. The plaques lie opposite a patch of muscle membrane of similar dimensions containing densely packed particles on the extracellular leaflet. Normal larval plaques average about 0.87 μm in length, and the presynaptic active zones are 0.22 μm long (Schaner and Rheuben, 1985). Typically, plaques are separated from each other along the nerve terminal by a substantial depression in which a glial process lies. Occasional deviations from this pattern have been seen in fifth-instar terminals. Two active zones may be found in the same plaque, and some apparent plaques have no obvious particle specialization to delineate an active zone. In other cases, the depression occupied by the glial process is absent, and adjacent plaques appear to be merging.

Degenerating terminals differ from normal ones by having, in addition to the plaques described above, a large number of plaques with active zones divided into short pieces or active zones whose particles are dispersed from the narrow band (Fig. 16). More plaques appear to be merging (Fig. 17), and more plaques have multiple, relatively short active zones than in normal muscle (Fig. 18B,C,D).

In some cases, plaques observed on the cytoplasmic leaflet contained several clusters of only three or four large particles. We were able to verify that some of the very small clusters of particles were short segments of active zones by examining the complementary replica of the extracellular leaflet, where the presence of a depression lined with pits and the scattered particles along that trough indicated that a short active zone actually was present.

In degenerating fibers, even very short fragments of active zones occasionally have fractured necks of what might be presumed to be exocytotic figures adjacent to them (Fig. 18), suggesting that transmitter release might still be possible at structurally abnormal active zones. In some fractures, large numbers of endocytotic figures are seen around the edges of the plaques. These occur in normal larval and adult muscle, particularly after nerve stimulation (Rheuben and Reese, 1978; Schaner and Rheuben, 1985).

Fig. 15. Low-magnification freeze-fracture view of a cytoplasmic leaflet of a nerve terminal from a fifth-instar larva. Portions of six plaques are shown. The three plaques whose active zones are indicated by arrows appear to be 'normal' (single active zone, about 0.2 μm long). The topmost plaque (asterisk) does not appear to have an active zone, and is identified as a plaque on the basis of the particle specializations on the pieces of postsynaptic membrane remaining around the edges. The plaque in the lower right-hand corner may have two active zones (arrowheads). 39 250×.

Freeze-fracture images including three or more adjacent plaques often showed that quite normal-looking plaques and active zones could occur immediately adjacent to very abnormal plaques and active zones (Fig. 16). This appeared to be the typical pattern of degeneration. We saw no examples of long fractures in which all active zones appeared to be abnormal or non-functional. However, the thin-section studies showed that some of the more degenerated junctions were attached to the muscle by a thin stalklike muscle process (Fig. 10). In complementary replicas (the method used here), the fracture plane largely runs in the smooth muscle membrane covering the bulk of the fiber and would be less likely to follow into a narrow neck connecting the junctional complex with the rest of the fiber. Consequently, the freeze-fracture data may be biased to include more normal or near-normal junctions in the sample.

Discussion

In both this study and in the companion paper describing the physiological observations (Sonea and Rheuben, 1992), we examined the degenerative changes that occur at the initiation of metamorphosis. The time was restricted to samples from the last days of the fifth instar (prepupal period) and the first 12 h after pupation. For certain quantitative questions, only fibers from day 1 pupae of specific ages were examined and compared to early fifth-instar (normal) fibers. In general, all those degenerative effects that could be seen clearly by day 1 of the pupal period could be observed to a lesser degree in the prepupae. During the first 12 h after pupation, the rate of degeneration appeared to be more rapid than during any comparable 12 h period in the prepupal period.

A number of interesting and unexpected physiological changes were documented for this period. Early day 1 pupae required lower Ca^{2+} concentrations to reduce EJPs below threshold for contraction than did normal larvae. Muscle fiber resting potentials began falling during the prepupal period and continued after ecdysis. The time courses of EJPs from degenerating day 1 pupal fibers were prolonged compared to those from larvae. While facilitation was not markedly affected, the ability to show long-term potentiation after high-frequency stimulation was reduced. There was an increased likelihood of observing conduction failure in peripheral nerves supplying the degenerating muscles.

Concomitant with these functional changes, we observed certain structural changes. Although there were degenerative changes in the nerve terminal, the

Fig. 16. Freeze-fracture view of a cytoplasmic leaflet of a nerve terminal from an AB fiber of a 6 h pupa. In this terminal, a normal active zone (arrow) is next to a plaque with a fragmented active zone (asterisks). 84 150×.

most striking changes occurred in the morphology of the glial cells, both those of the neuromuscular junction and those investing the nerve branches.

Changes in the motor nerves

The motor nerves undergo significant changes in structure during the early phase of metamorphosis. In a region which will continue to carry axons used in the adult, the glial cells swell and withdraw their processes from between the axons, leaving them adjacent to each other. During this time, the glial processes lose the high density of microtubules present in the larval nerves and which will reappear in the adult nerves. The peripheral 'collar' region of the nerve, with its thick neural lamella, is invaded by granulocytes or adipohemocytes as well as cells of unknown function. Similar changes have been reported by Pipa and Woolever (1965) for the interganglionic connectives of the moth *Galleria mellonella* and by McLaughlin (1974a) for the same region of *Manduca*. Pipa and Woolever suggest that the glial changes might be responsible for the shortening of the larval connectives that occurs. Our finding that similar glial reorganization occurs in the peripheral nerves and even in the distalmost tertiary muscle branches suggests that this may be a more general phenomenon associated with metamorphosis.

The nerves continue to conduct action potentials and to evoke an EJP up to about 12 h after the pupal ecdysis, as described by Sonea and Rheuben (1992). However, at high stimulus frequencies, conduction fails cyclically and intermittently in the degenerating nerves. All neurotransmission ceases abruptly rather than with gradually decreasing amplitudes of EJPs in pupal nerve–muscle preparations, suggesting that there might be inadequacies in function of the motor nerve, rather than gradual failure of the populations of junctions serving the observed muscle fiber.

The insect central nervous system is thought to be dependent upon a blood–brain barrier, constructed from layers of glial cells, for normal function because of the unusually high concentrations of K^+ and low concentrations of Na^+ in the hemolymph in some species (Pichon *et al.* 1972; Treherne and Schofield, 1981). McLaughlin (1974b) found in *Manduca* that the degree of penetration of the extracellular tracers lanthanum and peroxidase into the two perineurial glial layers of the central nervous system increased during metamorphosis. Although we have been unable to determine precisely which of the glial layers present in the peripheral nerves might correspond to the Types I and II perineurial layers that she describes in the central nervous system (McLaughlin, 1974a), the overall structural changes that we observed in the glia of the peripheral nerves are very similar. Consequently, the degenerating peripheral nerves may also have structural impairments of the glial layers which constitute their ionic barriers.

Furthermore, Treherne and Schofield (1981) suggest that ionic homeostasis is

17

Fig. 17. Freeze-fracture view of a cytoplasmic leaflet of a nerve terminal from an AB fiber of a 4 h pupa. The lower two plaques appear to have merged, with two active zones present, one fragmented (asterisks) and one shorter than typical (arrow). On the nerve terminal membrane, the borders of plaques are often demarcated by an increased density of small particles, as seen here. The distance between the two filled squares, the total length of the two fused plaques, was 1.64 μm. Such plaques could account for the long contact lengths seen in sectioned material (Fig. 14). The upper active zone (arrowheads) is more dishevelled than usual. 92050×.

not entirely dependent upon physical barriers, but also requires the presence of an extracellular matrix and a neuroglial cation transport system. During degeneration, the extracellular matrix surrounding the nerve appears to be phagocytosed by granular hemocytes, and any function it may have had in maintaining ionic homeostasis would be disrupted. A glial ion transport system might not function optimally if it were dependent upon metabolically derived components, since there is some evidence for changes in oxidative metabolism during metamorphosis (Bidlack and Lockshin, 1976). Consequently, the changes in glial cell morphology and physiology may directly or indirectly underlie the failure in neurotransmission at high stimulus frequencies if the appropriate ionic environment cannot be maintained adjacent to the motor axons.

Changes in the neuromuscular junction

It was important to determine the uniformity and timing of the degenerative changes in the neuromuscular junctions to compare the morphological results with those obtained electrophysiologically. An intracellular electrode records the composite signal from a large number of junctions on a single fiber because the space constant is long relative to the frequently distributed nerve terminals, but the fibers are several space constants in length. If degeneration were not uniform along the length of a fiber, the precise placement of the electrode would affect the observations. Randall and Pipa (1969) reported that degeneration was greater in the junctions closest to the cuticular attachments of the muscle fibers. In singly innervated frog muscle fibers, Birks *et al.* (1960) found that the degree of degeneration of the neuromuscular junctions was not uniform within a given muscle after denervation by nerve transection. Some individual junctions appeared functionally normal and others could produce neither an EJP nor miniature endplate potentials. In a similar preparation, Ko (1981) observed that all the active zones from a given terminal appeared disrupted, while those on an adjacent terminal might all appear normal. In *Manduca*, in contrast, we found that the junctions were consistently non-uniform with regard to the degree of degeneration along their lengths. Within a given junction, some regions of the nerve terminal maintained apparently normal contacts with the muscle, and other regions were clearly non-functional. Structurally normal active zones were found adjacent to abnormal ones in the same terminal. Like Ko (1981), we found evidence that the fragmented active zones could still release neurotransmitter,
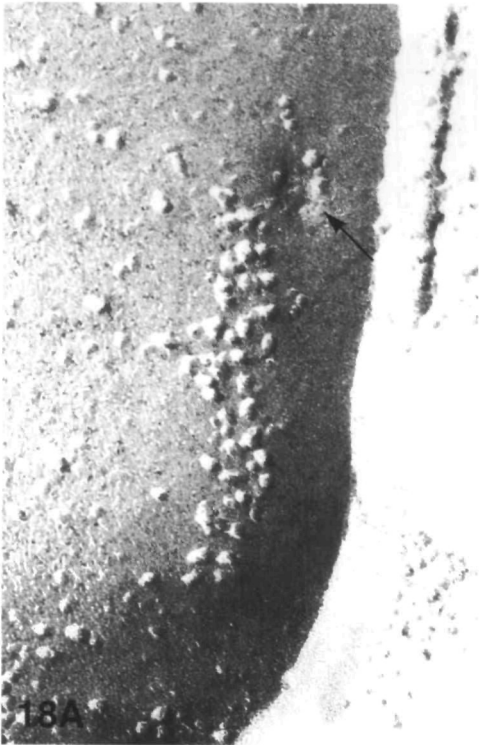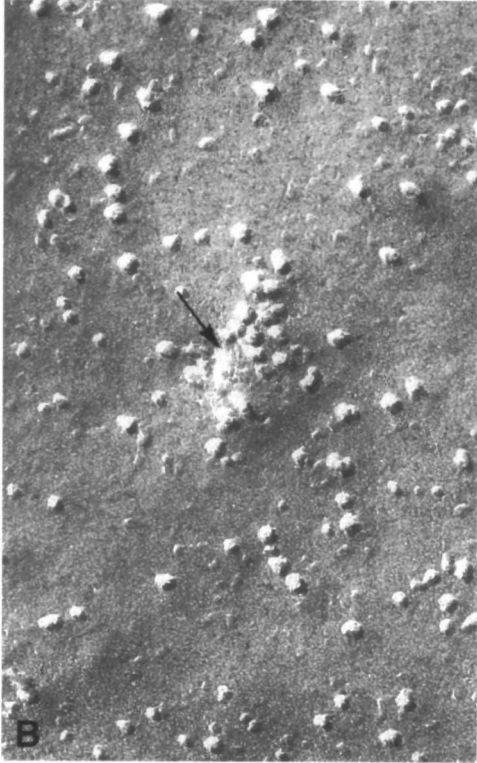
Fig. 18. Four active zones from fibers from a 6 h pupa, illustrating both normal (A) and abnormal (B–D) types. The active zone in D, which is divided into two parts, was from a plaque immediately adjacent to the lower (dishevelled) active zone in Fig. 16. The active zone in B is shorter than normal, and that in C is fragmented into several pieces; nevertheless, the fractures indicate the presence of exocytotic figures in both (arrows). These may indicate that evoked release is still possible from relatively abnormal active zones. 209 800×.

judging from the narrow necks of exocytotic profiles adjacent to them, but it is not known how this release might differ from normal.

No associations between degree of degeneration of the neuromuscular junction and location on a particular muscle fiber or on a group of fibers at a particular location were found, so we concluded that the populations of junctions which we were observing structurally, and from which we were recording (Sonea and Rheuben, 1992), were uniform. The morphological results were consistent with our previous physiological observations that an EJP could be recorded from virtually any muscle fiber, and that there was little change in amplitude of the EJP if the electrode was moved further up or down the muscle. Unlike most vertebrate skeletal muscles, insect muscle fiber membranes do not conduct action potentials, and distributed nerve endings are required to change the potential across the fiber uniformly and to induce contraction. Fairly uniform input from partly degenerated junctions could allow some degree of muscle function as metamorphosis progresses, and might have crucial importance for the shedding of the cuticle during the pupal ecdysis.

Structurally, the most striking change in the neuromuscular junction during degeneration is the systematic and apparently purposeful withdrawal of glial processes from the interstices of the junction. The glial cells do not appear to degenerate, at least not up to the time we have examined. In examples in which the nerve terminal has entirely withdrawn from the junction, the glial cells may encircle it. Whether this is a preliminary stage to phagocytosis is not yet determined.

Plasticity of glial structure within neuromuscular junctions has been observed in a variety of species. In denervated rat neuromuscular junctions (Miledi and Slater, 1968, 1970) the Schwann cell may engulf the nerve terminal and replace it over the endplate of the muscle and may be the source of miniature endplate potentials after the nerve has degenerated. In denervated cockroach muscle, there is hypertrophy and swelling of the glial profiles surrounding the nerve terminal (Wood and Usherwood, 1979). Signs of glial remodelling or degeneration have been reported in neuromuscular junctions of old mice (Ludatscher *et al.* 1985), following castration in the levator ani muscle of rats (Tobin and Pecot-Dechavassine, 1982) and in early adult junctions of the soleus muscle of rats (Cardasis and Padykula, 1981).

In the larval muscles of *Manduca* there are at least two implications of the withdrawal of the neuromuscular glial processes from the junction. The first, the

potential role of these cells in the subsequent development of the adult neuromuscular junction, remains to be explored. In the embryogenesis of *Manduca*, non-neural 'bridge' cells prefigure the pathway of the transverse nerves; the bridge cells later become glia ensheathing these axons (Carr and Taghert, 1988; Taghert *et al.* 1988). In the larval to adult transition a similar function for glial cells could reasonably be postulated.

The second implication of the glial withdrawal from the junction is the degree of plasticity in both structure and physiology of the remainder of the components of the junction that allow it to continue to function over several days. Contact between nerve terminal and muscle continues after glial withdrawal, and average contact lengths between nerve terminal membrane and muscle fiber postsynaptic processes increase. In some cases, the extra large contact areas seem to be fully occupied by typical electron-dense specializations within the postsynaptic membrane, presumably representing the presence of receptors. Larger areas occupied by receptors apposing each release site would be predicted to lead to a lengthening in the time course of synaptic currents (Wathey *et al.* 1979) and a subsequent lengthening of the excitatory junction potential, as was observed in many degenerating larval muscle fibers (Sonea and Rheuben, 1992). Fortier and Tremblay (1990) have noted a correlation between the longer time courses of miniature endplate currents in the proximal region of the frog neuromuscular junction and the longer postjunctional folds in this region.

The withdrawal of the glial processes might have another effect on the duration of synaptic currents. The uptake of glutamate from the synaptic cleft is thought to be a primary function of the junctional glia (Botham *et al.* 1979; Faeder and Salpeter, 1970). If the diffusion gradient out of the synaptic cleft were not maintained by the glial processes, repetitive binding of glutamate, particularly during prolonged stimulation, would also lengthen the duration of the synaptic currents. Consequently, the longer time courses of the intracellularly recorded EJPs could arise in part from prolonged synaptic currents. In addition, the electrotonic cable properties of the shrivelled muscle fiber and those of the peculiarly shaped postsynaptic apparatus in the degenerating junctions might influence both the time course and amplitude of the recorded EJP. Some quantitative predictions of these effects will be described in a subsequent article (M. B. Rheuben and S. M. Baer, in preparation). However, measurements of junctional currents will ultimately be necessary to separate pre- and postsynaptic phenomena.

Excitatory junction potentials were more difficult to reduce below the threshold for an active membrane response and contraction during the early phases of degeneration, requiring lower calcium concentrations than those needed for larval muscles (Sonea and Rheuben, 1992; I. M. Sonea, M. B. Rheuben and C. Young, in preparation). This is puzzling when one considers that, on average, 32–48 % of the profiles of nerve terminals from 0 to 13 h after pupation could be considered 'non-functional' from a structural viewpoint. If one-third to half of the active zones and postsynaptic specializations are not working properly, how could the EJP be

larger? The muscle fiber is undergoing severe atrophy at this time, but the expected increase in input resistance caused by the decrease in cross-sectional area and increase in surface membrane is calculated to be only 25 % (Rheuben, 1992) and may not be adequate to explain the difference. This question will be explored at a more quantitative level in a subsequent paper (M. B. Rheuben and S. M. Baer, in preparation) but, again, definitive solutions will require measurements of quantal content and synaptic currents.

In summary, the most striking findings include the degree to which glial changes influence the morphology and, presumably, the physiology of the degenerating neuromuscular junctions. The balance between remaining synaptic function and muscle fiber dimensions seems to allow the muscles to function even at quite an advanced stage of degeneration. The remarkable plasticity of the junction during degeneration suggests that some of these phenomena may also occur in both normal and developing junctions. Perhaps the number and size of plaques in junctions are controlled by the degree to which glial cells 'permit' contact between nerve and muscle, with contact by the nerve terminal eliciting development of the postsynaptic specialization.

References

BEAULATON, J. AND LOCKSHIN, R. (1978). Programmed cell death. Ultrastructural study of neuromuscular relations during degeneration of the intersegmental muscles. *Biol. Cellulaire* **33**, 169–174.

BIDLACK, J. M. AND LOCKSHIN, R. A. (1976). Evolution of LDH isozymes during programmed cell death. *Comp. Biochem. Physiol.* **55B**, 161–166.

BIRKS, R., KATZ, B. AND MILEDI, R. (1960). Physiological and structural changes at the amphibian myoneural junction, in the course of nerve degeneration. *J. Physiol., Lond.* **150**, 145–168.

BOTHAM, R. P., BEADLE, D. J., HART, R. J., POTTER, C. AND WILSON, R. G. (1979). Glutamate uptake after stimulation-induced depletion of vesicle numbers in neuromuscular junctions of *Locusta migratoria* L. *Cell Tissue Res.* **203**, 379–386.

CARDASIS, C. A. AND PADYKULA, H. A. (1981). Ultrastructural evidence indicating reorganization at the neuromuscular junction in the normal rat soleus muscle. *Anat. Rec.* **200**, 41–59.

CARR, J. N. AND TAGHERT, P. H. (1988). Formation of the transverse nerve in moth embryos. I. A scaffold of nonneuronal cells prefigures the nerve. *Devl Biol.* **130**, 487–499.

CASADAY, G. B. AND CAMHI, J. M. (1976). Metamorphosis of flight motor neurons in the moth *Manduca sexta*. *J. comp. Physiol.* **112**, 143–158.

FAEDER, I. R. AND SALPETER, M. M. (1970). Glutamate uptake by a stimulated insect nerve muscle preparation. *J. Cell Biol.* **46**, 300–307.

FORTIER, L. P. AND TREMBLAY, J. P. (1990). Postsynaptic structure may account for variations in miniature endplate current shapes along frog neuromuscular junctions. *Synapse* **5**, 255–264.

HEINERTZ, R. (1976). Untersuchungen am thorakalen Nervensystem von *Antheraea polyphemus* Cr. (Lepidoptera) unter besonderer Berucksichtigung der Metamorphose. *Rev. suisse Zool.* **83**, 215–242.

KO, C.-P. (1981). Electrophysiological and freeze-fracture studies of changes following degeneration at frog neuromuscular junctions. *J. Physiol., Lond.* **321**, 627–639.

LUDATSCHER, R. M., SILBERMANN, M., GERSHON, D. AND REZNICK, A. (1985). Evidence of Schwann cell degeneration in the aging mouse motor end-plate region. *Expl Geront.* **20**, 81–91.

MCLAUGHLIN, B. J. (1974a). Fine-structural changes in a lepidopteran nervous system during metamorphosis. *J. Cell Sci.* **14**, 369–387.

MCLAUGHLIN, B. J. (1974b). The accessibility of a developing lepidopteran nervous system to lanthanum and peroxidase. *J. Cell Sci.* **14**, 389–409.

MILEDI, R. AND SLATER, C. R. (1968). Electrophysiology and electron-microscopy of rat neuromuscular junctions after nerve degeneration. *Proc. R. Soc. Lond.* B **169**, 289–306.

MILEDI, R. AND SLATER, C. R. (1970). On the degeneration of rat neuromuscular junctions after nerve section. *J. Physiol., Lond.* **207**, 507–528.

PICHON, Y., SATTELLE, D. B. AND LANE, N. J. (1972). Conduction processes in the nerve cord of the moth *Manduca sexta* in relation to its ultrastructure and haemolymph ionic composition. *J. exp. Biol.* **56**, 717–734.

PIPA, R. L. AND WOOLEVER, P. S. (1965). Insect neurometamorphosis. II. The fine structure of perineurial connective tissue, adipohemocytes, and the shortening ventral nerve cord of a moth, *Galleria mellonella* (L.). *Z. Zellforsch. mikrosk. Anat.* **68**, 80–101.

RANDALL, W. C. AND PIPA, R. L. (1969). Ultrastructural and functional changes during metamorphosis of a proleg muscle and its innervation in *Galleria mellonella* (L.) (Lepidoptera: Pyralididae). *J. Morph.* **128**, 171–194.

REES, D. AND USHERWOOD, P. N. R. (1972). Fine structure of normal and degenerating motor axons and nerve–muscle synapses in the locust, *Schistocerca gregaria. Comp. Biochem. Physiol.* **43A**, 83–101.

RHEUBEN, M. B. (1992). Degenerative changes in the muscle fibers of *Manduca sexta* during metamorphosis. *J. exp. Biol.* **167**, 91–117.

RHEUBEN, M. B. AND KAMMER, A. E. (1980). Comparison of slow and fast adult muscle innervated by the same motor neurone. *J. exp. Biol.* **84**, 103–118.

RHEUBEN, M. B. AND REESE, T. S. (1978). Three-dimensional structure and membrane specializations of moth excitatory neuromuscular synapse. *J. Ultrastruct. Res.* **65**, 95–111.

SALPETER, M. M. AND FAEDER, I. R. (1971). The role of sheath cells in glutamate uptake by insect nerve muscle preparations. *Prog. Brain Res.* **34**, 103–114.

SCHANER, P. J. AND RHEUBEN, M. B. (1985). Scanning and freeze-fracture study of nerve and neuromuscular junctions in *Manduca sexta. J. Neurobiol.* **16**, 83–96.

SONEA, I. M. AND RHEUBEN, M. B. (1992). Degenerative changes in the function of neuromuscular junctions of *Manduca sexta* during metamorphosis. *J. exp. Biol.* **167**, 61–89.

STOCKER, R. F. AND NÜESCH, H. (1975). Ultrastructural studies on neuromuscular contacts and the formation of junctions in the flight muscle of *Antheraea polyphemus* (Lep.) I. Normal adult development. *Cell Tissue Res.* **159**, 245–266.

TAGHERT, P. H., CARR, J. N. AND WALL, J. B. (1988). The formation of a neurohaemal organ during insect embryogenesis. In *Advances in Insect Physiology*, vol. 20 (ed. P. D. Evans and V. B. Wigglesworth), pp.87–117. New York, London: Academic Press.

TOBIN, C. AND PECOT-DECHAVASSINE, M. (1982). Effect of castration on the morphology of the motor end-plates of the rat levator ani muscle. *Eur. J. Cell Biol.* **26**, 284–288.

TREHERNE, J. E. AND SCHOFIELD, P. K. (1981). Mechanisms of ionic homeostasis in the central nervous system of an insect. *J. exp. Biol.* **95**, 61–73.

WASSERMAN, A. J. (1985). Central and peripheral neurosecretory pathways to an insect flight motor nerve. *J. Neurobiol.* **16**, 329–345.

WATHEY, J. C., NASS, M. M. AND LESTER, H. A. (1979). Numerical reconstruction of the quantal events at nicotinic synapses. *Biophys. J.* **27**, 145–164.

WEEKS, J. C. AND TRUMAN, J. W. (1984). Neural organization of peptide-activated ecdysis behaviors during the metamorphosis of *Manduca sexta*. II. Retention of the proleg motor pattern despite loss of the prolegs at pupation. *J. comp. Physiol.* A **155**, 423–433.

WOOD, M. R. AND USHERWOOD, P. N. R. (1979). Ultrastructural changes in cockroach leg muscle following unilateral neurotomy. I. Degeneration. *J. Ultrastruct. Res.* **68**, 265–280.

YAMAMOTO, R. T. (1969). Mass rearing of the tobacco hornworm. II. Larval rearing and pupation. *J. econ. Ent.* **62**, 1427–1431.